Saudi Pharmaceutical Journal 31 (2023) 845–853

HOSTED BY

Contents lists available at ScienceDirect

Saudi Pharmaceutical Journal

journal homepage: www.sciencedirect.com

Original article

Encapsulation of morin in lipid core/PLGA shell nanoparticles significantly enhances its anti-inflammatory activity and oral bioavailability

Suhair Sunoqrot [a,*], Malak Alkurdi [a], Abdel Qader Al Bawab [a], Alaa M. Hammad [a], Rabab Tayyem [b], Ali Abu Obeed [b], Mohammed Abufara [b]

[a] Department of Pharmacy, Faculty of Pharmacy, Al-Zaytoonah University of Jordan, Amman 11733, Jordan
[b] ACDIMA Biocenter, Amman 11190, Jordan

ARTICLE INFO

Article history:
Received 18 November 2022
Accepted 7 April 2023
Available online 15 April 2023

Keywords:
Anti-inflammatory
Bioavailability
Morin
Nanoencapsulation
PLGA

ABSTRACT

Morin (3,5,7,2′,4′-pentahydroxyflavone; MR) is a bioactive plant polyphenol whose therapeutic efficacy is hindered by its poor biopharmaceutical properties. The purpose of this study was to develop a nanoparticle (NP) formulation to enhance the bioactivity and oral bioavailability of MR. The nanoprecipitation technique was employed to encapsulate MR in lipid-cored poly(lactide-co-glycolide) (PLGA) NPs. The optimal NPs were about 200 nm in size with an almost neutral surface charge and a loading efficiency of 82%. The NPs exhibited sustained release of MR within 24 h. In vitro antioxidant assays showed that MR encapsulation did not affect its antioxidant activity. On the other hand, anti-inflammatory assays in lipopolysaccharide-stimulated macrophages revealed a superior anti-inflammatory activity of MR NPs compared to free MR. Furthermore, oral administration of MR NPs to mice at a single dose of 20 mg/kg MR achieved a 5.6-fold enhancement in bioavailability and a prolongation of plasma half-life from 0.13 to 0.98 h. The results of this study present a promising NP formulation for MR which can enhance its oral bioavailability and bioactivity for the treatment of different diseases such as inflammation.

1. Introduction

Plant polyphenols are a group of chemically diverse compounds found in many herbs, fruits, and vegetables. These compounds have garnered a great deal of interest over the years for their notable anticancer, anti-inflammatory, antidiabetic, cardioprotective, and immunomodulatory properties (Abu Khalaf, 2016; Cory et al., 2018). Morin (3,5,7,2′,4′-pentahydroxyflavone; MR, Fig. 1) is one of the most important flavonoids isolated from the *Moraceae* family (Mottaghi and Abbaszadeh, 2021; Thakur et al., 2020). It is freely soluble in organic solvents but less soluble in water, with an absolute oral bioavailability of<1% (Choi et al., 2015; Ikeuchi-Takahashi et al., 2020). The absorption process of poorly water-soluble drugs is limited by their dissolution, which consequently impacts their oral bioavailability. Despite MR's poor solubility, it has several health benefits such as antioxidant (Zhao et al., 2019), anti-inflammatory (Kuzu et al., 2018), anticancer (Hwang-Bo et al., 2019), free radical scavenging (Veerappan et al., 2019), antidiabetic (Razavi et al., 2019), antimicrobial (de Farias et al., 2021), and neuroprotective (Mu et al., 2021) effects.

Polymeric nanoparticles (NPs) have sparked a lot of interest in recent years because of their unique properties that can overcome the delivery challenges of poorly soluble drug candidates. NPs have the potential for a wide range of applications, including targeted drug delivery, controlled release, protection of drug molecules, and improved therapeutic index (Crucho and Barros, 2017). Polymeric NPs have been employed as delivery systems for various synthetic and natural drugs to improve their effectiveness and bioavailability (Pridgen et al., 2015). They can be fabricated from different types of polymers, among which poly(lactide-co-glycolide) (PLGA) is particularly popular (Fig. 1). Besides being approved by the US Food and Drug Administration (FDA), it is

* Corresponding author at: Department of Pharmacy, Faculty of Pharmacy, Al-Zaytoonah University of Jordan, P.O. Box 130, Amman 11733, Jordan.
E-mail address: suhair.sunoqrot@zuj.edu.jo (S. Sunoqrot).

Peer review under responsibility of King Saud University.

Production and hosting by Elsevier

https://doi.org/10.1016/j.jsps.2023.04.010
1319-0164/

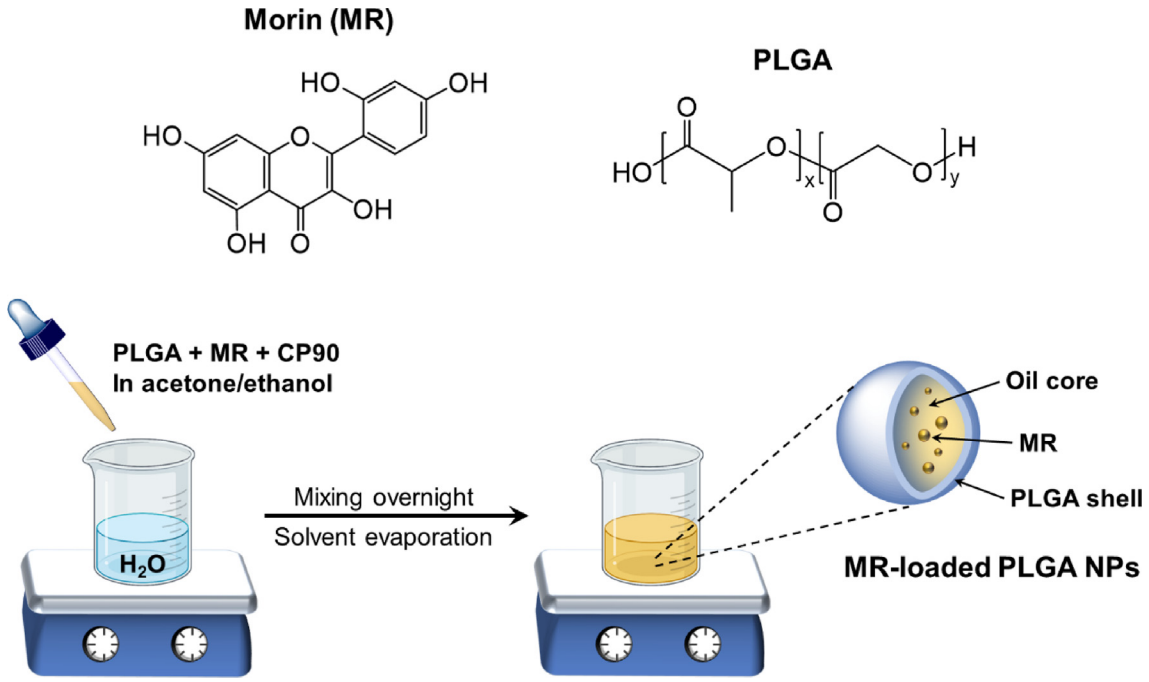

Fig. 1. Structures of MR and PLGA and an overview of MR NPs fabrication by nanoprecipitation to obtain NPs with an oil-filled core and a polymeric shell.

biodegradable, biocompatible, and may be tailored to form various polymeric delivery systems such as NPs, microspheres, and implants (Sur et al., 2019).

Despite its promising therapeutic benefits, there have been only a few reports involving the application of nanotechnology-based platforms for the delivery of MR. Examples include solid lipid NPs (Ikeuchi-Takahashi et al., 2016; Karamchedu et al., 2020), nanoemulsions (Ikeuchi-Takahashi et al., 2020), micelles (Choi et al., 2015), and polymeric NPs based on hydroxyethyl starch (Li et al., 2018) and hyaluronic acid-poly (butyl cyanoacrylate) (Abbad et al., 2015). One report described the development of PLGA-based NPs for dermal delivery of MR as a sunscreen adjuvant with an encapsulation efficiency of 12% (Shetty et al., 2015). Another study investigated the interaction between MR-loaded PLGA NPs and human serum albumin, with no focus on a particular therapeutic application. Both studies used the emulsion-solvent evaporation technique to fabricate the NPs, which typically involves significant energy input in the form of high frequency ultrasound during NP preparation. On the other hand, the nanoprecipitation technique requires minimal energy input as it relies on mixing the water-miscible organic phase containing the polymer and drug with water at a controlled rate (Martínez Rivas et al., 2017). A modification on the classic technique has emerged where an oil may be added to the organic phase, and with the aid of hydrophilic and lipophilic surfactants, the polymer can precipitate as nanocapsules with a lipophilic core/polymeric shell architecture (Martínez Rivas et al., 2017; Masood, 2016; Mora-Huertas et al., 2010). This type of NPs offers advantages over conventional matrix-type NPs such as enhanced drug loading in the lipid core and improved physical and biological stability because of the presence of a polymer shell. This formulation approach has been successfully applied for the encapsulation of plant polyphenols such as quercetin (El-Gogary et al., 2014), baicalin (El-Gogary et al., 2019), and cirsiliol (Al-Shalabi et al., 2020), as well as other plant-derived bioactive compounds such as curcumin (Klippstein et al., 2015) and thymoquinone (Sunoqrot et al., 2020). However, no such approach has been attempted to deliver MR.

In this study, we set out to investigate whether entrapping MR in PLGA NPs could enhance its anti-inflammatory activity and bioavailability, since most of the reported MR nanoformulations focused on its anticancer activity, and the bioavailability of PLGA-based MR formulations has not been previously evaluated. MR was encapsulated in lipid core/PLGA shell NPs by nanoprecipitation. Following physicochemical characterization, the NPs were tested for *in vitro* antioxidant and anti-inflammatory activities and *in vivo* absorption after oral administration to healthy mice.

2. Experimental section

2.1. Materials

MR was obtained from TCI (Japan). PLGA (lactide/glycolide ratio of 50:50 and MW of 5–10 kDa) was obtained from Acros Organics (Fisher Scientific, USA). Span 80 and 2,2-diphenyl-1-picrylhydrazyl (DPPH) were procured from Sigma-Aldrich (USA). Dimethyl sulfoxide (DMSO), potassium bromide (KBr), acetone (absolute) and ethanol (absolute) were purchased from Fisher Chemical (UK). Capryol 90 (CP90) was a kind gift from Gattefossé (France). Olive oil (extra virgin) was purchased from a local supermarket (Jordan). Castor oil (BP) was obtained from Philadelphia Pharmaceuticals (Jordan). Tween 80 was obtained from RFCL Ltd (India). Phosphate buffered saline (PBS, 10×) was purchased from Fisher Bioreagents (Belgium). Lipopolysaccharide (LPS; E. coli O55:B5) was obtained from Santa Cruz Biotechnology Inc. (USA). Type 1 ultrapure water was used throughout the experiments.

2.2. Encapsulation of MR in lipid core/PLGA shell NPs

MR was encapsulated in PLGA NPs with a lipid core and a polymeric shell following a previously described method with some modification (Sunoqrot et al., 2020). First, the solubility of MR was tested in three different oils: olive oil, castor oil, and CP90. Fifty milligrams of MR were placed in a glass vial, to which 1 mL of each oil was added. The vials were vortexed for 30 sec and then placed in an orbital shaking incubator (Biosan ES-20, Latvia)

operating at room temperature and 200 rounds per minute (rpm). The samples were incubated for 24 h, after which the contents of each vial were transferred to 1.5 mL microtubes and centrifuged at 4000 × g for 5 min (Hermle Z326K centrifuge, Germany) to separate the undissolved solid. Then, a sample of each supernatant was diluted ten times in DMSO and the amount of MR dissolved in each oil was determined by UV–Vis (UV-1800, Shimadzu, Japan) based on a calibration curve of MR absorbance at 358 nm versus concentration. Having shown the highest solubilization capacity for MR, CP90 was chosen as the lipid core for the NPs. For the encapsulation of MR in the NPs, PLGA (25 mg) and MR (2.5 mg or 5 mg) were co-dissolved in 5 mL of acetone/ethanol (60:40, v/v), to which CP90 (150 µL) and Span 80 (25 mg) were added as the lipid core and the lipophilic surfactant, respectively. The organic phase was sonicated in a bath sonicator for 10 min. Meanwhile, the aqueous phase was prepared which consisted of 10 mL 0.2% Tween 80 in water as a hydrophilic surfactant. The organic phase was dropped into the aqueous phase under stirring (400 rpm), then the NP dispersion was stirred under ambient conditions overnight to allow for the evaporation of the organic solvents. The NPs were purified by ultrafiltration as previously described (Al-Shalabi et al., 2020; Sunoqrot et al., 2020) and were stored at 4 ^{o}C until further characterization.

2.3. Measurement of particle size and zeta potential

Dynamic light scattering was employed to determine the particle size and polydispersity index (PDI) of MR NPs using a Nicomp® Nano Z3000 instrument (Entegris, USA). Measurements were conducted at 25 ^{o}C and a scattering angle of 90^{o}. Samples were diluted 1:1 in ultrapure water prior to the measurements. Zeta potential measurements were acquired using the same instrument in the zeta potential mode.

2.4. Determination of encapsulation efficiency (EE)

To determine the encapsulation efficiency (EE) of MR, freshly purified NPs were diluted ten times in DMSO to dissolve all the NP ingredients. The total amount of MR within the NPs was determined by UV–Vis as described previously (Mondal et al., 2022). The UV absorbance of MR was measured at 358 nm (λ_{max} for MR in DMSO), and the concentration of MR present in the NPs was extrapolated from a calibration curve of MR absorbance at 358 nm versus concentration. The concentration was multiplied by the total volume of the NP dispersion, giving the amount of encapsulated MR, then EE% was calculated according to Eq. (1):

$$\text{Encapsulation efficiency (EE\%)} = \frac{\text{Actual amount of encapsulated drug (mg)}}{\text{Initial amount of drug added (mg)}} \times 100\% \quad (1)$$

2.5. Fourier transform-infrared (FT-IR) spectroscopy characterization

MR NPs were mixed with KBr and dried over night at 40 °C. The powder was then pressed into a pellet for FT-IR analysis. MR and PLGA (as powders) were prepared directly as KBr pellets. Spectra were acquired using an IR Affinity-1 spectrometer (Shimadzu, Japan).

2.6. Transmission electron microscopy (TEM) imaging

The NPs were visualized by transmission electron microscopy (TEM) to determine their morphology. Briefly, 10 µL of fresh NPs was placed on TEM grids and left for 1 min. The excess liquid was blotted with filter paper, and the grids were imaged as previously described (Sunoqrot et al., 2022).

2.7. In vitro release of MR from MR NPs

The release of MR from MR NPs was evaluated in PBS pH 7.4 to mimic physiologic conditions and in 0.1 N HCl to simulate the gastric environment. One milliliter of fresh MR NPs was aliquoted in a dialysis membrane (12–14 kDa MWCO, Spectra/Por 2, Repligen, USA) in triplicate and immersed in 30 mL 0.1 N HCl or PBS supplemented with 0.5% w/v Tween 80 to maintain sink conditions (Sunoqrot et al., 2020). Free MR (1 mL, 0.5 mg/mL in DMSO) was also tested for comparison. The samples were placed in an orbital shaking incubator (37 °C, 100 rpm). At specific time intervals, samples of the release medium were withdrawn and exchanged with an equivalent volume of fresh release medium. The amount of drug released was determined by UV–Vis, and the release profile was plotted from the percentage ratio of the cumulative quantity of drug released at each time interval to the total amount of drug in the NPs versus time (h).

2.8. Antioxidant activity of MR NPs

The antioxidant activity of MR NPs was determined by a DPPH assay and compared to the antioxidant activity of free MR. For the assay, serial dilutions (1.6–200.0 µg/mL) were prepared for each material in DMSO. Then, 200 µL of each dilution was mixed with 4 mL of DPPH (0.1 mM in ethanol). The samples were well mixed and incubated at room temperature in the dark for 30 min. The absorbance of the samples was then read at 517 nm. Antioxidant activity was calculated based on Eq. (2):

$$\text{Antioxidant activity (\%)} = [(A_{DMSO} - A_{sample})/A_{DMSO}] \times 100\% \quad (2)$$

where A_{sample} is the absorbance after incubating the sample with DPPH, and A_{DMSO} is the absorbance of DMSO with DPPH (blank). The experiment was performed on three different NP batches and the results were reported as the mean ± SD.

2.9. In vitro anti-inflammatory assay in lipopolysaccharide (LPS)-stimulated RAW 264.7 macrophages

The RAW 264.7 cell line was obtained from the American Type Culture Collection (ATCC, USA) and maintained as described previously (Al-Shalabi et al., 2022). The anti-inflammatory assay was conducted in lipopolysaccharide (LPS)-stimulated RAW 264.7 macrophages by measuring the concentration of nitrite which corresponds to the concentration of nitric oxide (NO) released from the cells due to LPS-induced oxidative stress. For the experiment, cells were seeded in 96-well plates at a density of 10,000 cells/well and allowed to attach overnight. The next day, the anti-inflammatory assay was conducted as previously described with some modification (Schmölz et al., 2017). Briefly, cells (n = 5) were treated with 0–50 µM free MR (from a 20 mg/mL stock solution in DMSO) or MR NPs diluted in 100 µL complete culture medium for 4 h (the concentration range was chosen so as to maintain at least 80% cell viability). Blank NPs (without MR) were also included at equivalent concentrations to MR NPs. Then, the media was removed and replaced with fresh media containing 1 µg/mL LPS, and the cells were further incubated for 20 h (24 h total incubation time). Another group of cells remained untreated and was not stimulated with LPS to serve as the negative control. After the end of the incubation period, 50 µL from each well was transferred to a new 96-well plate, followed by adding 50 µL of the Griess reagent (Sigma-Aldrich, USA) to each well. Sodium nitrite standards (Sigma-Aldrich, USA) were also prepared between 0 and

100 μM and 50 μL of each standard was mixed with 50 μL of the Griess reagent in the same 96-well plate. After incubation for 10 min at room temperature in the dark, the absorbance of the plate was read at 540 nm (Synergy HTX multi-mode microplate reader, Biotek, USA). The amount of nitrite in the cell supernatants was calculated based on the calibration curve of the sodium nitrite standards' absorbance at 540 nm versus concentration. The results were reported as the mean ± SD of the 5 replicate wells for each concentration.

2.10. In vivo bioavailability of MR NPs after oral administration

The animal protocol for this study was authorized by the Animal Care and Use Committee of Al-Zaytoonah University of Jordan (decision no. 1/5/2021–2022), and was conducted in accordance with the Helsinki guidelines for animal research. Thirty-six male Balb/c mice (8–10 weeks old) were kept in plastic cages with free access to food and drink, and they were fasted overnight before the experiment. The mice were divided into two groups of 18 mice each. Animals in group 1 were administered a single dose of 20 mg/kg MR dissolved in a mixture of PEG 400 and ultrapure water (1:3 v/v) by oral gavage. Animals in group 2 were administered a single dose of 20 mg/kg of MR NPs in ultrapure water (equivalent dose to free MR) through oral gavage. At 0.25, 0.5, 1, 2, 4 and 6 h after dose administration, 3 mice from each group were euthanized by diethyl ether and cervical dislocation, and blood was collected from the jugular vein into heparinized microtubes. Blood samples were kept at room temperature for 20 min and were then centrifuged at 5000 rpm for 20 min. Five hundred microliters of plasma was collected from each sample and stored at − 80 °C until further analysis.

2.11. Determination of MR plasma levels via liquid chromatography-tandem mass spectrometry (LC-MS/MS)

Instrumentation.

The concentration of MR in plasma samples was analyzed based on a previously reported method (Choi et al., 2015). The separation was performed on an Agilent 1260 series LC system equipped with an autosampler and an in-line degasser, and coupled with an Applied Biosystems API 4000 mass spectrometer detector (Sciex, Canada). Samples (10 μL) were eluted on an Eclipse XDB C18 column (4.6 × 150 mm, 5 μm) using a mobile phase consisting of acetonitrile and water (50:50 v/v) with 0.1% formic acid delivered isocratically at a flow rate of 1 mL/min, and the column temperature was kept at 40 °C. Mass spectra were acquired by electrospray ionization in the positive mode. Quantification was performed using selected reaction monitoring (SRM) at m/z 301.1 → 151.0 for MR and m/z 364.0 → 223.0 for amoxicillin (internal standard).

2.11.1. Preparation of calibration curve samples

An MR stock solution was prepared by dissolving 5 mg MR in 50 mL methanol to obtain a final concentration of 0.1 mg/mL. The MR stock solution was serially diluted in the mobile phase to obtain MR standard solutions, which were then spiked into blank plasma from untreated mice to obtain the calibration curve samples with concentrations ranging between 10 and 850 ng/mL.

2.11.2. Preparation of plasma samples

Seventy-five microliters of plasma were added to 400 μL methanol containing 20 μL of amoxicillin internal standard (150 μg/mL in methanol). After vortex-mixing for 1 min, the samples were centrifuged for 5 min at 3700 × g. The supernatant (10 μL) was then injected directly into the LC-MS/MS system. The concentration of MR in each sample was determined from the calibration curve standards and plotted against time (h) to obtain the plasma profile. Pharmacokinetic parameters (t_{max} and C_{max}) were determined directly from the plasma concentration–time curves. The plasma half-life ($t_{0.5}$) was obtained by fitting the elimination phase time points to the first-order equation ($Log\ C = Log\ C_{max} - kt/2.303$), where $t_{0.5} = 0.693/k$. The area under the curve ($AUC_{0\rightarrow tlast}$) for each group was calculated in GraphPad Prism 7. AUC values for the two groups were compared according to the Bailer method (Bailer, 1988) at an $\alpha = 0.05$ and a $Z_{crit} = 2.24$. Z_{obs} was calculated according to the Eq. (3):

$$Z_{obs} = \frac{AUC_{MR} - AUC_{MR\ NPs}}{\sqrt{s^2 AUC_{MR} + s^2 AUC_{MR\ NPs}}} \quad (3)$$

where the null hypothesis H_0: $AUC_{MR} = AUC_{MR\ NPs}$ would be rejected if $|Z_{obs}| \geq Z_{crit}$.

2.12. Statistical analysis

All reported values represent the mean ± SD of at least three independent experiments. Unless otherwise indicated, means were compared by one-way or two-way analysis of variance (ANOVA), followed by Tukey or Sidak's multiple comparisons tests, respectively, where $p < 0.05$ was considered statistically significant.

3. Results and discussion

3.1. Preparation of MR-loaded NPs

MR was encapsulated in lipid core/PLGA shell NPs using the nanoprecipitation technique (Fig. 1), which was employed due to its convenience and simplicity. The classic method leads to the formation of nanospheres where the loaded drug is entrapped within a homogenous polymer matrix as the organic phase is exchanged with the aqueous phase (Martínez Rivas et al., 2017). The method has been adapted to produce reservoir-type NPs with a core/shell architecture by incorporating oils in the organic phase and adding hydrophilic and lipophilic surfactants in the organic and aqueous phases, respectively (Mora-Huertas et al., 2010). This approach has previously been shown to improve drug loading capacity for polymeric NPs compared to conventional matrix-type NPs (Sunoqrot et al., 2020). To choose a suitable lipid for NP preparation, the solubility of MR was assessed in three biocompatible oils: olive oil, castor oil (previously used by our group and others for the encapsulation of bioactive natural compounds in polymeric NPs), and CP90 (a lipophilic excipient used in oral lipid-based formulations). The solubility of MR in the three oils was in the order of: olive oil (practically insoluble) < castor oil (5.7 mg/mL) < CP90 (41.5 mg/mL). Based on these results, CP90 was used to form the lipid core of the NPs.

The NPs were primarily characterized in terms of particle size, polydispersity, and EE%. As noted in Table 1, when MR was added at 2.5 mg (10% of the polymer weight), MR NPs (F1) achieved a high EE of 82%. However, when the amount was increased to 5 mg (F2), EE decreased to 57%, implying that the loading capacity of the NPs had been exceeded. The two NP formulations were similar with regard to particle size, PDI, and zeta potential. F1 NPs were around 205 nm in size, whereas F2 NPs were slightly larger at 266 nm and more broadly distributed. Both formulations exhibited a PDI of around 0.30 which indicated moderate polydispersity. Surface charge as measured by the zeta potential was employed as an estimate of the colloidal stability of MR NPs. The electrostatic repulsion between particles can have a significant impact on the stability of NPs in a colloidal dispersion. It is also a main factor responsible for their interaction with the cell membrane, which is typically negatively charged. The average zeta potential for MR NPs was almost neutral, most likely due to the persistence of

Table 1
Characteristics of MR-loaded NPs (mean ± SD; n = 3).

Formula no.	MR (mg)	Particle size* (nm)	PDI	Zeta-potential (mV)	EE%
F1	2.5	205 ± 42	0.33 ± 0.04	−1.5 ± 1.4	82 ± 8
F2	5.0	266 ± 109	0.28 ± 0.13	−0.9 ± 1.7	57 ± 8

* Intensity-weighted.

nonionic surfactants (Span 80 and Tween 80) near the NP surface, which also can contribute to their colloidal stability, similar to previous results (Al-Shalabi et al., 2020; Sunoqrot et al., 2020). Having shown a superior EE%, F1 NPs were selected for subsequent experiments.

FT-IR was used to identify chemical functional groups in MR NPs compared to PLGA and MR powder. The FT-IR spectrum of free MR exhibited a broad O–H stretching band between 3000 and 3700 cm^{-1} corresponding to its polyphenolic structure (Fig. 2A). PLGA showed several characteristic bands: C=O stretching at 1700 cm^{-1} corresponding to the ester carbonyl groups, C–H stretching at 2900 cm^{-1} corresponding to the lactide/glycolide backbone, and weak O–H stretching at 3600 cm^{-1} corresponding to the terminal –OH groups. A broad O–H stretching band also appeared in the FT-IR spectrum of MR NPs between 3000 and 3700 cm^{-1}, but it was lower in intensity compared to free MR, suggesting that MR was entrapped inside the PLGA NPs. The spectrum also revealed the C=O and C–H stretching bands of PLGA at 1700 and 2900 cm^{-1}, respectively. Overall, the FT-IR spectrum of MR NPs did not reveal any incompatibilities between MR and PLGA as no new peaks appeared. The TEM image of MR NPs (F1) is presented in Fig. 2B, where the NPs appeared as dark spheres surrounded by a lighter rim, consistent with their core/shell structure.

3.2. In vitro release of MR from MR-loaded NPs

MR release from the NPs was studied in PBS (pH 7.4) and in 0.1 N HCl at 37 °C up to 96 h. Samples were withdrawn at different time intervals to determine the cumulative amount of MR released over time (Fig. 3A). Free MR was released from the dialysis membrane relatively quickly regardless of the pH of the release medium, reaching 92 and 100% release within 8 and 24 h, respectively. On the other hand, the release profile of MR NPs in the two media was biphasic, with a steady increase in cumulative drug release within the first 8 h and a slower release pattern up to 96 h. Release in 0.1 N HCl was relatively slower that in PBS, with 5% cumulative release after 1 h, increasing to 20% and 36% after 4 and 8 h, respectively. By 24 h, around 61% was released, and release was completed by 96 h. As for release at neutral pH, around 18% of MR was released after 1 h of incubation, which gradually increased to 58% and 84% after 4 and 8 h, respectively. By 24 h, MR achieved 92% cumulative release, and reached 99% by 96 h of incubation. Although release in PBS was faster than in 0.1 N HCl for MR NPs, it was significantly slower than the diffusion of the free drug within the first 24 h (Fig. 3B), confirming the sustained release characteristics of the formulation. In addition, the slow drug release in the acidic medium simulating the gastric environment will ensure that sufficient drug is available for intestinal absorption *in vivo*. Drug release could be explained by drug diffusion across the oil core through the polymer shell and concurrent polymer erosion (Kamaly et al., 2016). The results were in agreement with previous findings where hydrophobic drugs such as thymoquinone and baicalin were each encapsulated within NPs with an oil-filled core and a polymeric shell and exhibited similar release kinetics (El-Gogary et al., 2019; Sunoqrot et al., 2020).

3.3. Antioxidant activity of MR NPs

Like other molecules in its class, MR is known to possess prominent antioxidant activity due to its ability to scavenge reactive species and neutralize free radicals by virtue of its highly conjugated aromatic structure and the presence of multiple hydroxyl groups (Caselli et al., 2016; Marković et al., 2012). To determine whether the encapsulation of MR could preserve its antioxidant activity, a DPPH assay was conducted on MR-loaded NPs and free MR in parallel, by monitoring the absorbance of the DPPH radical. The assay

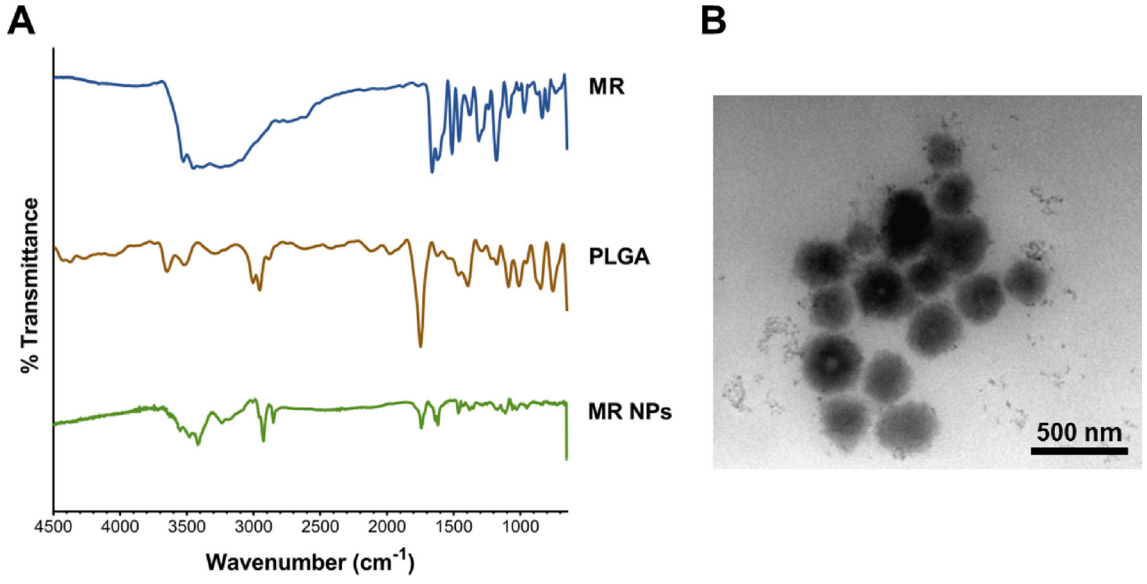

Fig. 2. (A) FT-IR spectra of MR, PLGA and MR NPs (F1); (B) TEM image of MR NPs (F1).

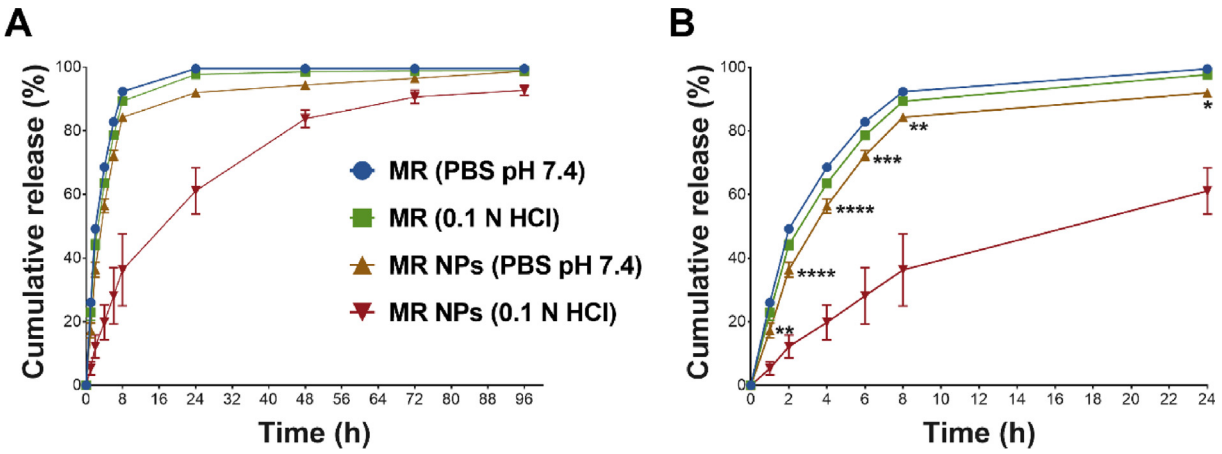

Fig. 3. In vitro release of MR from NPs studied in PBS pH 7.4 and 0.1 N HCl at 37 °C. Free MR was added for comparison. (A) Release profiles up to 96 h; (B) Expanded release profiles during the first 24 h. Results are expressed as the average % cumulative release ± SD (n = 3) versus time (h). *$p < 0.05$, **$p < 0.01$, ***$p < 0.001$, and ****$p < 0.0001$ compared to free MR in PBS pH 7.4 based on one-way ANOVA followed by Tukey's multiple comparisons test.

works on the principle that a substance with antioxidant activity will transfer an electron to quench the DPPH radical, resulting in a decrease in absorbance at 517 nm (λ_{max} for the DPPH radical). Thus, the decrease in the DPPH radical absorbance, which is relative to the quantity of antioxidant, is used as an indication of radical scavenging activity. Fig. 4 shows the % antioxidant activity of different concentrations of free MR and MR NPs (1.6–200.0 μg/mL). The results showed no significant difference between the two forms, indicating that MR NPs had similar antioxidant activity compared to the free drug, and that the encapsulation process did not compromise MR's free radical scavenging activity. The results are consistent with a previous report where the bioactive plant polyphenol cirsiliol was formulated in lipid-cored polymeric NPs which preserved its antioxidant activity (Al-Shalabi et al., 2020).

3.4. In vitro anti-inflammatory activity of MR NPs

The anti-inflammatory activity of MR NPs was evaluated using RAW 264.7 macrophages stimulated with LPS. The activity was determined based on the concentration of nitrite released from the cells, which can be conveniently detected by the Griess reagent. Cells were treated with different concentrations of MR NPs and equivalent concentrations of free MR for 4 h, followed by stimulation with LPS for 20 h before measuring nitrite levels (Schmölz et al., 2017). As shown in Fig. 5, LPS caused a significant increase in nitrite concentration in untreated cells. Free MR had no effect on reducing nitrite levels at all the tested concentrations (6.25–50 μM). However, MR NPs showed a significant reduction in nitrite levels starting from the lowest concentration (6.25 μM). In fact, the nitrite concentration in cells treated with MR NPs was similar to the control (unstimulated cells). We noticed that the highest concentration of MR NPs (50 μM) started to show an increase in nitrite concentration, which may be due to increased oxidative stress caused by the high polymer mass. However, the nitrite concentration was not significantly different from the control (unstimulated cells) and from the blank NPs. The difference between free MR and MR NPs is most likely because of the enhanced intracellular delivery of MR NPs compared to free MR due to its low water solubility. Similar results were observed for rhoifolin, a bioactive plant polyphenol with potent antioxidant activity, where rhoifolin-entrapped PLGA NPs of similar size and morphology to MR NPs significantly improved its intracellular antioxidant activity by facilitating its cellular uptake (Al-Shalabi et al., 2022). Another study reported that rutin loaded in liquid crystalline NPs around 200 nm in diameter and with a spherical morphology reduced the inflammatory response to LPS in human bronchial epithelial cells more effectively than the free compound, most likely by promoting its cellular uptake (Paudel et al., 2020).

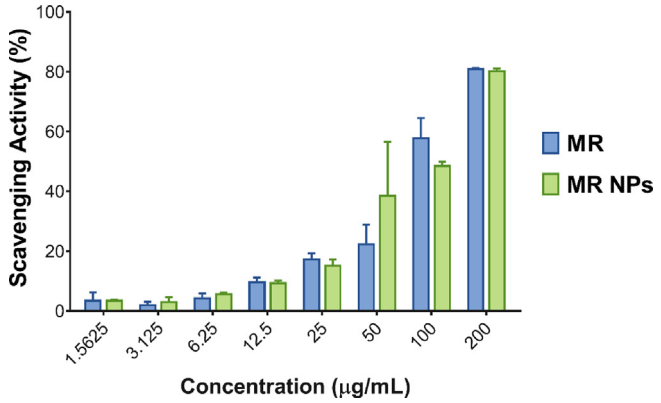

Fig. 4. Antioxidant activity of MR NPs compared to free MR as revealed by the DPPH assay. Results are expressed as the % DPPH radical scavenging activity versus MR concentration (μg/mL) (n = 3). Results were compared by unpaired *t*-test which found no significant differences between the two groups at all the tested concentrations.

3.5. In vivo bioavailability of MR NPs after oral administration

MR is reported to have an absolute oral bioavailability of less than 1% (Zhang et al., 2011), which is largely attributed to its poor aqueous solubility. Nanotechnology-based delivery systems have the potential to enhance drug delivery through the oral route, especially for drugs suffering from low solubility. Having shown potent anti-inflammatory activity *in vitro*, MR NPs were considered as a promising formulation to test *in vivo* to investigate the potential enhancement in oral bioavailability, since the oral route is the most convenient route of administration. In a pilot pharmacokinetic study, animals were given MR NPs or free MR as a single oral dose of 20 mg/kg. Each time point, 3 animals from each group were euthanized and their plasma was collected to analyze the concentration of MR by LC-MS/MS. Plasma concentrations versus time for the two groups were plotted and analyzed by GraphPad Prism 7 to calculate the pharmacokinetic parameters such as C_{max} (highest concentration of drug in the blood after it is given), t_{max} (the time

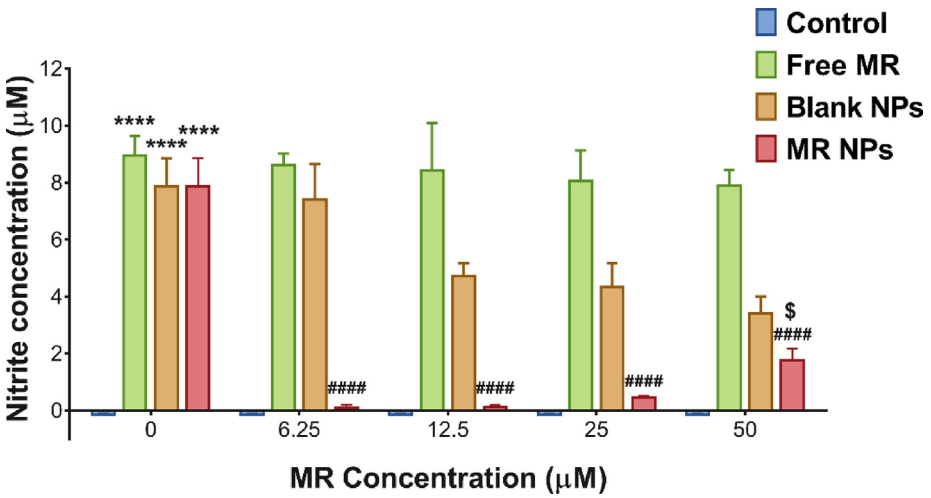

Fig. 5. Anti-inflammatory activity of MR and MR NPs in LPS-stimulated RAW 264.7 macrophages indicated by measuring the concentration of nitrite in the cell culture medium of treated cells. Blank NPs were added for comparison. $^{****}p < 0.0001$ compared to the control (unstimulated cells), $^{\#\#\#\#}p < 0.0001$ compared to free MR and blank NPs, and $^{\$}p < 0.05$ compared to blank NPs based on 2-way ANOVA followed by Tukey's multiple comparisons test (n = 5).

it takes for the drug to reach the C_{max}), $t_{0.5}$ (the time required for the plasma concentration to decrease by 50%), and $AUC_{0\rightarrow tlast}$ (the area under the plasma concentration–time curve from t = 0 till t = 6 h). As shown in Fig. 6 and Table 2, free MR achieved a C_{max} of 2667 ng/mL at 0.25 h (15 min) post administration. On the other hand, MR NPs started appearing in the plasma at 0.25 h. Nonetheless, the NPs were able to achieve a higher C_{max} of 4157 ng/mL at 0.5 h. This delay may be attributed to the slower absorption of the NPs compared to the free drug in the gastrointestinal tract. The higher C_{max} is likely due to the enhanced solubility and permeability of MR mediated by the NPs.

After reaching the C_{max}, plasma levels of free MR immediately started to decrease, reaching the lowest value of 39 ng/mL after 6 h. As for the NPs, the plasma concentration decreased at a slower rate. Even after 6 h, the concentration was still high at 809 ng/mL. As a result, $t_{0.5}$ for MR NPs was prolonged to 0.98 h compared to 0.13 h for free MR. The $AUC_{0\rightarrow tlast}$ of MR NPs was significantly greater than that obtained for free MR as confirmed by Bailer's AUC equality test ($|Z_{obs}| > Z_{crit}$). As shown in Table 2, the AUC for MR NPs was 5.6 times greater than free MR ($p < 0.05$ based on unpaired t-test). Collectively, these results indicate that the NP formulation could significantly improve the extent of drug absorption and prolong the duration the drug remains in the blood. Interestingly, a similar NP formulation was used to load thymoquinone, and the NPs showed only 30% improvement in oral bioavailability compared to the free drug. In addition, the half-lives for free thymoquinone and the NP form were similar (Sunoqrot et al., 2020). Here we saw a more significant enhancement in bioavailability and prolongation of the half-life, which may be due to sustained release of the drug from the NPs, as well as the enhanced solubility and permeability. The results were consistent with previous findings related to MR (Choi et al., 2015; Zhang et al., 2011) and other

Table 2
Pharmacokinetic parameters after oral administration of 20 mg/kg free MR and MR NPs to mice. Results are reported as the mean ± SD (n = 3).

Parameter	MR	MR NPs
C_{max} (ng/mL)	2667 ± 543	4157 ± 2081
t_{max} (h)	0.25	0.5
$t_{0.5}$ (h)	0.13	0.98
$AUC_{0\rightarrow tlast}$ (ng.h/mL)	1294 ± 331	7306* ± 1609

* Denotes statistical significance ($p < 0.05$) based on unpaired t-test.

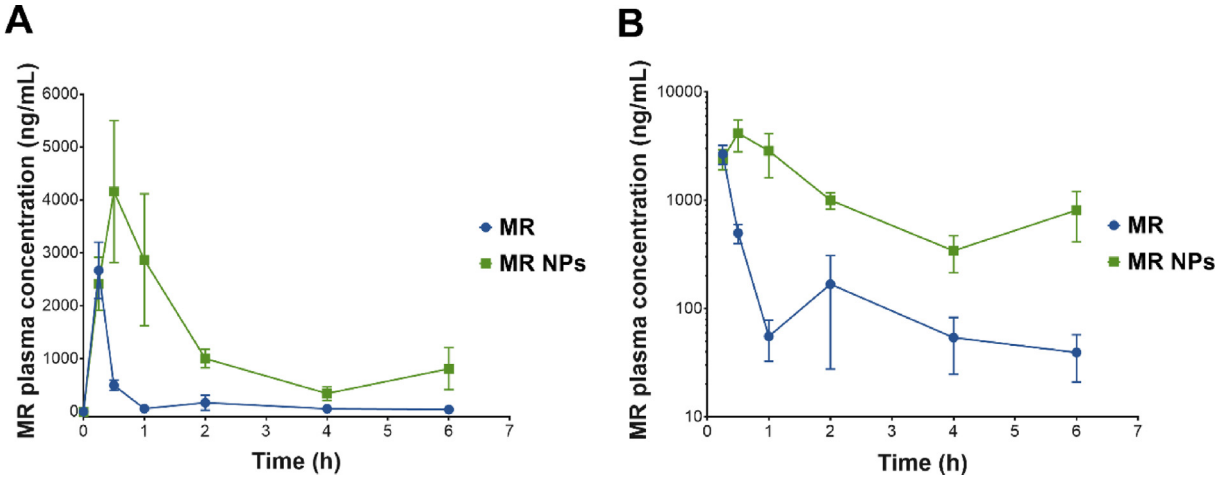

Fig. 6. (A) Plasma concentrations versus time profiles of MR following oral administration to mice as free MR or MR NPs at 20 mg/kg (n = 3); (B) The same plasma concentrations versus time profiles plotted on a logarithmic y-scale to highlight the elimination phase.

plant polyphenols such as quercetin (Penalva et al., 2017) and curcumin (Ban et al., 2020) when formulated in various nanocarriers.

MR has not been extensively evaluated *in vivo*. Only a few studies mention applying MR in animals, because it suffers from low bioavailability orally. Most studies have used intravenous (IV) administration, for example to evaluate the cancer targeting ability of MR NPs (Abbad et al., 2015) and for hyperuricemia treatment (Li et al., 2018). Another study used gold NPs-loaded MR liposomes but the nanocarrier in this case was not 100% biodegradable (Ding et al., 2020). Other reports have used formulations such as surfactant micelles composed of Pluronic F127 and Tween 80 (Choi et al., 2015) and phospholipid nanoemulsions (Zhang et al., 2011) for oral administration. In our study, we developed NPs using the biodegradable polymer PLGA and biocompatible components, achieving sustained release and improved oral absorption, which can be advantageous to benefit from MR's bioactivity, for example in inflammatory conditions.

4. Conclusions

Herein we encapsulated MR in lipid core/PLGA shell NPs by the nanoprecipitation method. The NPs achieved an EE of 82%, a particle size around 200 nm with good polydispersity, and an almost neutral surface charge. The NPs were further characterized by FT-IR and *in vitro* release. The release was sustained during the first 8 h and completed by 96 h. In vitro antioxidant activity showed that the encapsulation of MR did not significantly affect its free radical scavenging activity. In vitro anti-inflammatory activity in LPS-stimulated macrophages revealed that the MR NPs were superior to free MR in reducing the inflammatory response. A pilot *in vivo* pharmacokinetic study was conducted in mice to examine the bioavailability of MR NPs after a single oral dose. The study highlighted the superior performance of the NP formulation which achieved a dramatic improvement in bioavailability and a prolongation of the plasma half-life compared to the free drug. Altogether, our results present a promising nanotechnology-based formulation strategy that not only can potentiate the activity of MR but also facilitate its oral administration.

Declaration of Competing Interest

The authors declare that they have no known competing financial interests or personal relationships that could have appeared to influence the work reported in this paper.

Acknowledgements

This work received financial support from Al-Zaytoonah University of Jordan [grant no. 14/08/2021-2022]. The authors thank Lujain Alzaghari and Samah Abusulieh (Al-Zaytooonah University of Jordan) for assistance with the animal experiments and the *in vitro* release tests.

References

Abbad, S., Wang, C., Waddad, A.Y., Lv, H., Zhou, J., 2015. Preparation, in vitro and in vivo evaluation of polymeric nanoparticles based on hyaluronic acid-poly (butyl cyanoacrylate) and D-alpha-tocopheryl polyethylene glycol 1000 succinate for tumor-targeted delivery of morin hydrate. Int. J. Nanomedicine 10, 305–320.

Abu Khalaf, R., 2016. Exploring natural products as a source for antidiabetic lead compounds and possible lead optimization. Curr. Top. Med. Chem. 16, 2549–2561.

Al-Shalabi, E., Alkhaldi, M., Sunoqrot, S., 2020. Development and evaluation of polymeric nanocapsules for cirsiliol isolated from Jordanian *Teucrium polium* L. as a potential anticancer nanomedicine. J. Drug Deliv Sci. Technol. 56, 101544.

Al-Shalabi, E., Abusulieh, S., Hammad, A.M., Sunoqrot, S., 2022. Rhoifolin loaded in PLGA nanoparticles alleviates oxidative stress and inflammation in vitro and in vivo. Biomater. Sci. 10, 5504–5519.

Bailer, A.J., 1988. Testing for the equality of area under the curves when using destructive measurement techniques. J. Pharmacokinet. Biopharm. 16, 303–309.

Ban, C., Jo, M., Park, Y.H., Kim, J.H., Han, J.Y., Lee, K.W., Kweon, D.-H., Choi, Y.J., 2020. Enhancing the oral bioavailability of curcumin using solid lipid nanoparticles. Food Chem. 302, 125328.

Caselli, A., Cirri, P., Santi, A., Paoli, P., 2016. Morin: a promising natural drug. Current Medicinal Chemistry 23, 774–791.

Choi, Y.A., Yoon, Y.H., Choi, K., Kwon, M., Goo, S.H., Cha, J.-S., Choi, M.-K., Lee, H.S., Song, I.-S., 2015. Enhanced oral bioavailability of morin administered in mixed micelle formulation with Pluronic F127 and Tween 80 in rats. Biol. Pharm. Bull. 38, 208–217.

Cory, H., Passarelli, S., Szeto, J., Tamez, M., Mattei, J., 2018. The role of polyphenols in human health and food systems: A mini-review. Front. Nutr. 5, 87.

Crucho, C.I.C., Barros, M.T., 2017. Polymeric nanoparticles: A study on the preparation variables and characterization methods. Mater. Sci. Eng. C 80, 771–784.

de Farias, A.L., Arbeláez, M.I.A., Meneguin, A.B., Barud, H.d.S., Brighenti, F.L., 2021. Mucoadhesive controlled-release formulations containing morin for the control of oral biofilms. Biofouling, 1–13.

Ding, X., Yin, C., Zhang, W., Sun, Y., Zhang, Z., Yang, E., Sun, D., Wang, W., 2020. Designing aptamer-gold nanoparticle-loaded pH-sensitive liposomes encapsulate morin for treating cancer. Nanoscale Res. Lett. 15, 68.

El-Gogary, R.I., Rubio, N., Wang, J.-T.-W., Al-Jamal, W.T., Bourgognon, M., Kafa, H., Naeem, M., Klippstein, R., Abbate, V., Leroux, F., Bals, S., Van Tendeloo, G., Kamel, A.O., Awad, G.A.S., Mortada, N.D., Al-Jamal, K.T., 2014. Polyethylene glycol conjugated polymeric nanocapsules for targeted delivery of quercetin to folate-expressing cancer cells in vitro and in vivo. ACS Nano 8, 1384–1401.

El-Gogary, R.I., Gaber, S.A.A., Nasr, M., 2019. Polymeric nanocapsular baicalin: Chemometric optimization, physicochemical characterization and mechanistic anticancer approaches on breast cancer cell lines. Sci. Rep. 9, 11064.

Hwang-Bo, H., Lee, W.S., Nagappan, A., Kim, H.J., Panchanathan, R., Park, C., Chang, S. H., Kim, N.D., Leem, S.H., Chang, Y.C., 2019. Morin enhances auranofin anticancer activity by up-regulation of DR4 and DR5 and modulation of Bcl-2 through reactive oxygen species generation in Hep3B human hepatocellular carcinoma cells. Phytother. Res. 33, 1384–1393.

Ikeuchi-Takahashi, Y., Ishihara, C., Onishi, H., 2016. Formulation and evaluation of morin-loaded solid lipid nanoparticles. Biol. Pharm. Bull., b16–00300

Ikeuchi-Takahashi, Y., Murata, S., Murata, W., Kobayashi, A., Ishihara, C., Onishi, H., 2020. Development of Morin-Loaded Nanoemulsions Containing Various Polymers; Role of Polymers in Formulation Properties and Bioavailability. AAPS PharmSciTech 21, 1–11.

Kamaly, N., Yameen, B., Wu, J., Farokhzad, O.C., 2016. Degradable controlled-release polymers and polymeric nanoparticles: Mechanisms of controlling drug release. Chem. Rev. 116, 2602–2663.

Karamchedu, S., Tunki, L., Kulhari, H., Pooja, D., 2020. Morin hydrate loaded solid lipid nanoparticles: Characterization, stability, anticancer activity, and bioavailability. Chem. Phys. Lipids. 233, 104988.

Klippstein, R., Wang, J.-T.-W., El-Gogary, R.I., Bai, J., Mustafa, F., Rubio, N., Bansal, S., Al-Jamal, W.T., Al-Jamal, K.T., 2015. Passively Targeted Curcumin-Loaded PEGylated PLGA Nanocapsules for Colon Cancer Therapy In Vivo. Small 11, 4704–4722.

Kuzu, M., Kandemir, F.M., Yildirim, S., Kucukler, S., Caglayan, C., Turk, E., 2018. Morin attenuates doxorubicin-induced heart and brain damage by reducing oxidative stress, inflammation and apoptosis. Biomed. Pharmacother. 106, 443–453.

Li, J., Yang, Y., Lu, L., Ma, Q., Zhang, J., 2018. Preparation, characterization and systemic application of self-assembled hydroxyethyl starch nanoparticles-loaded flavonoid Morin for hyperuricemia therapy. Int. J. Nanomedicine 13, 2129–2141.

Marković, Z., Milenković, D., Đorović, J., Dimitrić Marković, J.M., Stepanić, V., Lučić, B., Amić, D., 2012. PM6 and DFT study of free radical scavenging activity of morin. Food Chem. 134, 1754–1760.

Martínez Rivas, C.J., Tarhini, M., Badri, W., Miladi, K., Greige-Gerges, H., Nazari, Q.A., Galindo Rodríguez, S.A., Román, R.Á., Fessi, H., Elaissari, A., 2017. Nanoprecipitation process: From encapsulation to drug delivery. Int. J. Pharm. 532, 66–81.

Masood, F., 2016. Polymeric nanoparticles for targeted drug delivery system for cancer therapy. Mater. Sci. Eng. C 60, 569–578.

Mondal, S., Das, S., Mahapatra, P.K., Saha, K.D., 2022. Morin encapsulated chitosan nanoparticles (MCNPs) ameliorate arsenic induced liver damage through improvement of the antioxidant system and prevention of apoptosis and inflammation in mice. Nanoscale Adv. 4, 2857–2872.

Mora-Huertas, C.E., Fessi, H., Elaissari, A., 2010. Polymer-based nanocapsules for drug delivery. Int. J. Pharm. 385, 113–142.

Mottaghi, S., Abbaszadeh, H., 2021. The anticarcinogenic and anticancer effects of the dietary flavonoid, morin: Current status, challenges, and future perspectives. Phytother. Res. 35, 6843–6861.

Mu, L., Hui, C., Li, W., 2021. Morin provides neuroprotection in a model of cerebral infarction via Nrf-2 signaling pathway. Curr. Top. Nutraceutical Res. 19.

Paudel, K.R., Wadhwa, R., Mehta, M., Chellappan, D.K., Hansbro, P.M., Dua, K., 2020. Rutin loaded liquid crystalline nanoparticles inhibit lipopolysaccharide induced oxidative stress and apoptosis in bronchial epithelial cells in vitro. Toxicol. In Vitro 68, 104961.

Penalva, R., González-Navarro, C.J., Gamazo, C., Esparza, I., Irache, J.M., 2017. Zein nanoparticles for oral delivery of quercetin: Pharmacokinetic studies and

preventive anti-inflammatory effects in a mouse model of endotoxemia. Nanomedicine 13, 103–110.
Pridgen, E.M., Alexis, F., Farokhzad, O.C., 2015. Polymeric nanoparticle drug delivery technologies for oral delivery applications. Expert Opin. Drug Deliv. 12, 1459–1473.
Razavi, T., Kouhsari, S.M., Abnous, K., 2019. Morin exerts anti-diabetic effects in human HepG2 cells via down-regulation of miR-29a. Exp. Clin. Endocrinol. Diabetes 127, 615–622.
Schmölz, L., Wallert, M., Lorkowski, S., 2017. Optimized incubation regime for nitric oxide measurements in murine macrophages using the Griess assay. J. Immunol. Methods 449, 68–70.
Shetty, P.K., Venuvanka, V., Jagani, H.V., Chethan, G.H., Ligade, V.S., Musmade, P.B., Nayak, U.Y., Reddy, M.S., Kalthur, G., Udupa, N., Rao, C.M., Mutalik, S., 2015. Development and evaluation of sunscreen creams containing morin-encapsulated nanoparticles for enhanced UV radiation protection and antioxidant activity. Int. J. Nanomedicine 10, 6477–6491.
Sunoqrot, S., Alfaraj, M., Hammad, A.a.M., Kasabri, V., Shalabi, D., Deeb, A.A., Hasan Ibrahim, L., Shnewer, K., Yousef, I., 2020. Development of a thymoquinone polymeric anticancer nanomedicine through optimization of polymer molecular weight and nanoparticle architecture. Pharmaceutics 12.
Sunoqrot, S., Aliyeh, S., Abusulieh, S., Sabbah, D., 2022. Vitamin E TPGS-poloxamer nanoparticles entrapping a novel PI3Kα inhibitor potentiate its activity against breast cancer cell lines. Pharmaceutics 14, 1977.
Sur, S., Rathore, A., Dave, V., Reddy, K.R., Chouhan, R.S., Sadhu, V., 2019. Recent developments in functionalized polymer nanoparticles for efficient drug delivery system. Nano-Struct. Nano-Objects 20, 100397.
Thakur, K., Zhu, Y.-Y., Feng, J.-Y., Zhang, J.-G., Hu, F., Prasad, C., Wei, Z.-J., 2020. Morin as an imminent functional food ingredient: An update on its enhanced efficacy in the treatment and prevention of metabolic syndromes. Food Funct. 11, 8424–8443.
Veerappan, I., Sankareswaran, S.K., Palanisamy, R., 2019. Morin protects human respiratory cells from PM2.5 induced genotoxicity by mitigating ROS and reverting altered miRNA expression. Int. J. Environ. Res. Public Health 16.
Zhang, J., Peng, Q., Shi, S., Zhang, Q., Sun, X., Gong, T., Zhang, Z., 2011. Preparation, characterization, and in vivo evaluation of a self-nanoemulsifying drug delivery system (SNEDDS) loaded with morin-phospholipid complex. Int. J. Nanomedicine 6, 3405.
Zhao, L.-J., Yang, S.-L., Jin, W., Yang, H.-W., Li, F.-Y., Chi, S.-M., Zhu, H.-Y., Lei, Z., Zhao, Y., 2019. Host-guest inclusion systems of morin hydrate and quercetin with two bis (β-cyclodextrin) s: Preparation, characterization, and antioxidant activity. Aust. J. Chem. 72, 440–449.